PHOTOMASK

BACUS—The international technical group of SPIE dedicated to the advancement of photomask technology.

September 2014
Volume 30, Issue 9

Best Poster - EMLC14

Black Border, Mask 3D effects: covering challenges of EUV mask architecture for 22 nm node and beyond

Natalia Davydova, Eelco van Setten, Robert de Kruif, Ramasubramanian Kottumakulal Jaganatharaja, Ad Lammers, Dorothe Oorschot, Cheuk-Wah Man, Guido Schiffelers, and Joep van Dijk, ASML Netherlands B.V., De Run 6501, 5504 DR Veldhoven, The Netherlands

Brid Connolly, Toppan Photomasks inc., Rähnitzer Allee 9, 01109 Dresden, Germany

Norihito Fukugami, Yutaka Kodera, Hiroaki Morimoto, Yo Sakata, Jun Kotani, and Shinpei Kondo, and Tomohiro Imoto, Toppan Printing Co., Ltd. Nobidome 7-21-33, Niiza, Saitama, 352-8562 Japan

Haiko Rolff and Albrecht Ullrich, AMTC GmbH & Co. KG, Raehnitzer Allee 9, D-01109 Dresden, Germany

ABSTRACT

Photomask is at the heart of a lithographic scanner's optical path. It cannot be left non-optimized from the imaging point of view. In this work we provide new insights on two critical aspects of EUV mask architecture: optimization of absorber for 16 nm half-pitch imaging and a systematic approach to black border EUV and DUV reflectance specifications.

Good 16 nm imaging is demonstrated on ASML NXE:3300 EUV scanner. Currently a relatively high dose resist is used for imaging and the dose reduction is desired. Optimization (reduction) of absorber height and mask CD bias can allow for up to 30% dose reduction without essential contrast loss. Disadvantages of absorber height reduction are ~7 nm increase of best focus range through pitch and tighter absorber height mean to target and uniformity requirements. A disadvantage of a smaller reticle CD (down to 14 nm 1x) is manufacturing process uniformity over the reticle.

A systematic approach of black border reflections impact on imaging is established. The image border is a pattern free dark area surrounding the image field and preventing exposure of the image field neighborhood on wafer. Currently accepted design of the black border on EUV reticle

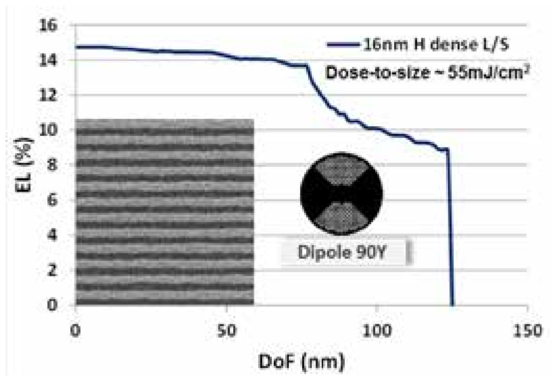

Figure 1. 16 nm line/spaces (LS) imaging results, NXE:3300, Dipole 90 Y illumination.

Take A Look Inside:

Industry Briefs
—see page 13

Calendar
For a list of meetings
—see page 14

SPIE.

EMLC14-BEST POSTER

Editorial

EUV Defect Free, is actinic the only solution?

Paul Morgan, Micron Technology Inc.

As we travel this difficult road we call EUV, we have been challenged with many opportunities (engineer speak for problems that we can turn into features) that may still be considered insurmountable. Of ALL of these challenges I see three primary ones I call the EUV version of Cerberus; Source Power, Time, and Defectivity. All three must be overcome for us to succeed. Leaving Time and Source Power to other technology warriors, I can only address Defectivity as the focus of my efforts and with that I propose the question "Is EUV the first reticle node to require actinic patterned aerial Inspection?"

We are constantly reminded through the various symposia, seminars, panels, papers, and peer discussions that we still have a long way to go to enable EUV. We have defectivity sourced from blank manufacturing, process manufacturing, shipping, handling, and even scanner operation all contributing to this challenge. Overcoming these sources of defectivity may require unique, novel, and perhaps overly complicated solutions (translation: expensive). The variety of these solutions may be overwhelming but if we drill down to another level of the problem statement, a single consideration may nullify many of these solutions; "Does a zero height multilayer defect exist, and can the positional accuracy of actinic blank inspection allow for the proposed repair strategies?" What is a zero height multi-layer defect and can it exist? I believe it is any defect in the multilayer that does not change the shape of the surface but modifies the illumination. I'm not sure that is the clearest answer, but this assumption drives current decision making.

Reticle inspection has been dominated by two strategies, High Resolution inspection and Aerial Inspection at both actinic (the wavelength the reticle will be used to expose wafers on a wafer Scanner) and non-actinic wavelength. Each has its strengths and weaknesses that may require subsequent processing that addresses the obvious question, does this defect cause a failure? Once we are aware of the defect we can then apply a variety of repair strategies that can be validated through repeated inspection or aerial review. With EUV we may have the same post detection strategy as current reticle technology, repair and review, the aerial review being EUV actinic (13.5nm.) The tooling to accomplish this will be available but given the nature of a zero height multilayer defect and the potential positional inaccuracy of an actinic blank inspection, current or proposed future non-actinic inspection strategies may not be able to answer the question of defect performance because you will not even be aware (of the defects existence) to ask it.

A challenge to this would be, what if we use wafer print as the final inspection for an EUV reticle? This would provide all of the detail necessary to identify the defects that "matter". Afterward, the reticle could be repaired using proposed EUV repair strategies and then the repair could be reviewed and the whole process would work! Maybe, besides the timing and coordination involved, a few added complications appear. Again we have the positional accuracy in the wafer inspection to where the defect is in the reticle pattern (keep thinking zero height) may be insufficient and additionally, how do you discriminate the post reticle manufacturing sourced defects. A blocked contact is a blocked contact, unless you find the fall-on after the reticle has been returned to the reticle manufacturer. Not wanting to provide additional support for the EUV pellicle effort but we may not have a choice.

Getting back to the primary issue, can you detect the defects that matter in your EUV process? If the defectivity is what we consider "normal" process related defects or contamination, then the obvious answer is yes, but if the distribution and exposure sensitivity of these multilayer defects is such that they do not change the topography of the surface then high resolution or E-Beam inspection may be insufficient. Which goes back to the original question, do we need actinic pattern inspection for EUV? Each of us has either already answered that question, or needs to get going - and soon.

N • E • W • S

BACUS News is published monthly by SPIE for BACUS, the international technical group of SPIE dedicated to the advancement of photomask technology.

Managing Editor/Graphics Linda DeLano
Advertising Lara Miles
BACUS Technical Group Manager Pat Wight

■ 2014 BACUS Steering Committee ■

President
Frank E. Abboud, *Intel Corp.*

Vice-President
Paul W. Ackmann, *GLOBALFOUNDRIES Inc.*

Secretary
Bryan S. Kasprowicz, *Photronics, Inc.*

Newsletter Editor
Artur Balasinski, *Cypress Semiconductor Corp.*

2014 Annual Photomask Conference Chairs
Paul W. Ackmann, *GLOBALFOUNDRIES Inc.*
Naoya Hayashi, *Dai Nippon Printing Co., Ltd.*

International Chair
Uwe F. W. Behringer, *UBC Microelectronics*

Education Chair
Artur Balasinski, *Cypress Semiconductor Corp.*

Members at Large
Paul C. Allen, *Toppan Photomasks, Inc.*
Michael D. Archuletta, *RAVE LLC*
Peter D. Buck, *Mentor Graphics Corp.*
Brian Cha, *Samsung*
Glenn R. Dickey, *Shin-Etsu MicroSi, Inc.*
Brian J. Grenon, *Grenon Consulting*
Thomas B. Faure, *IBM Corp.*
Jon Haines, *Micron Technology Inc.*
Mark T. Jee, *HOYA Corp, USA*
Oliver Kienzle, *Carl Zeiss SMS GmbH*
Patrick M. Martin, *Applied Materials, Inc.*
M. Warren Montgomery, *The College of Nanoscale Science and Engineering (CNSE)*
Wilbert Odisho, *KLA-Tencor Corp.*
Michael T. Postek, *National Institute of Standards and Technology*
Abbas Rastegar, *SEMATECH North*
Emmanuel Rausa, *Plasma-Therm LLC.*
Douglas J. Resnick, *Canon Nanotechnologies, Inc.*
Thomas Struck, *Infineon Technologies AG*
Bala Thumma, *Synopsys, Inc.*
Jacek K. Tyminski, *Nikon Research Corp. of America (NRCA)*
Jim N. Wiley, *ASML US, Inc.*
Larry S. Zurbrick, *Agilent Technologies, Inc.*

SPIE.

P.O. Box 10, Bellingham, WA 98227-0010 USA
Tel: +1 360 676 3290
Fax: +1 360 647 1445
www.SPIE.org
help@spie.org

©2014

All rights reserved.

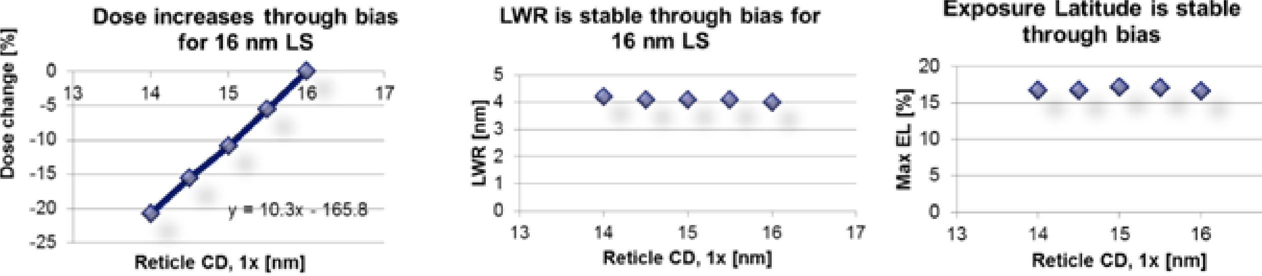

Figure 2. Imaging performance of 16 nm LS through bias. (Left) Imaging dose to target reduces by 10% per 1 nm negative line CD bias. (Center) LWR is stable through bias. (Right) Exposure latitude is stable through bias.

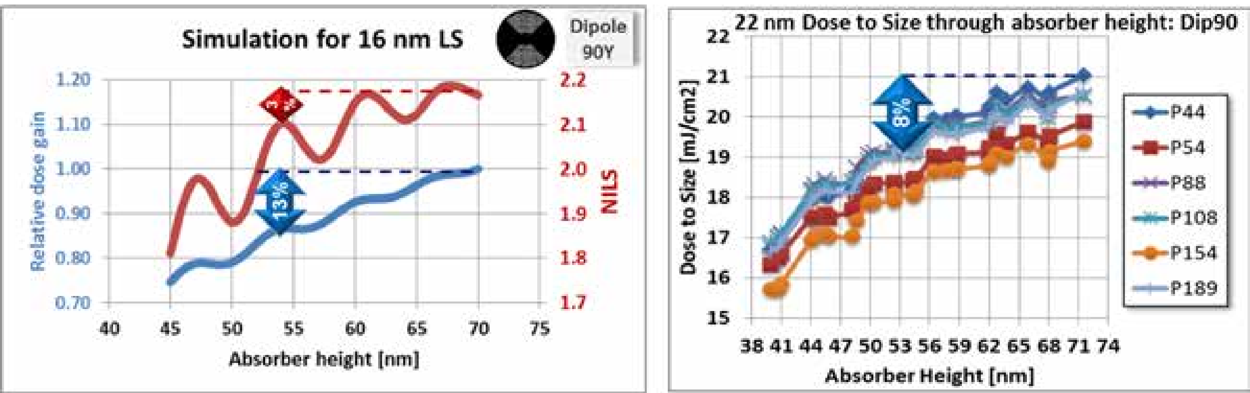

Figure 3. (Left) 16 nm LS imaging simulation through AH, Dipole 90Y illumination, NXE:3300 settings. AH reduction from 70 nm to 54 nm allows for 13% dose gain with only 3% NILS reduction. (Right) Experimental results[7] of 22 nm imaging through pitch and AH on NXE:3300 with Dipole 90Y illumination. AH reduction from 72 nm to 53 nm allows for 8% dose gain for dense lines.

is an image border where the absorber and multilayer stack are etched down to the substrate and EUV reflectance is reduced to <0.05%. DUV reflectance of such a black border is about 5%. It is shown that a tighter DUV reflectance specification <1.5% is required driven by the impact of DUV reflections from the black border on imaging. NXE:3300 and NXE:3100 experimental imaging results are shown. The need of low DUV wavelength reflectance metrology (in the range 100-300 nm) is demonstrated using an estimated NXE scanner out-of-band DUV spectrum. Promising results of low DUV reflectance of the black border are shown.

1. Introduction

In this work we provide new insights on two critical aspects of EUV mask architecture. In the first part optimization of absorber for 16 nm half-pitch imaging is considered. The main goal is to investigate potential imaging dose reduction by means of absorber height (AH) and critical dimension (CD) bias reduction.

In the second part a systematic approach to black border (BB) EUV and DUV reflectance specifications is explored based on experimental results of DUV level measurements and imaging results on NXE:3100 and NXE:3300 scanners.

2. Absorber Optimization for 16 nm Imaging

2.1. 16 nm imaging on NXE:3300

Good 16 nm line/spaces (LS) imaging results are demonstrated on ASML NXE:3300 EUV scanner[1][2][3][4] showing large process window with exposure latitude above 14% and depth of focus above 120 nm (Figure 1). Relative high dose resist is used with imaging dose of about 55 mJ/cm^2.[2] Dose reduction is desired for higher throughput. No special mask optimization was done so far for the dose reduction: 70 nm AH mask was used and no line CD bias was applied to imaging features.

2.2. Negative line CD bias allows for 20% dose gain

There is a general simple rule: the smaller the absorber volume on the mask, the smaller the dose needed for the exposure. One

Table 1. ITRS (2013) requirements for AH control.

	2013	2014	2015	2016	2017
Absorber film thickness uniformity (nm, 3 sigma) [P]	0.57	0.52	0.48	0.44	0.40
Attenuated PSM absorber thickness mean to target (± % of target) [W]	1.4	1.4	1.4	1.4	1.4
Attenuated PSM absorber thickness uniformity (% of target, range) [X]	1.1	1.1	1.1	1.1	1.1

Table 2. ITRS and ASML requirements for 70 and 53 nm absorber mask. Tighter requirements might be needed for 53 nm absorber mask.

Target AH	70 nm	53 nm	53 nm tight reqs
ITRS Absorber film thickness (AH) uniformity in 2015 (nm, 3sigma)	0.48	0.48	
ITRS Attenuated PSM absorber thickness mean to target (± 1.4% of target, nm)	0.98	0.74	
ITRS Attenuated PSM absorber thickness uniformity (±1.1% of target, nm, range)	0.77	0.58	
ASML AH mean to target (± nm)	1.0	1.0	**0.5**
ASML AH variation (± 1% of target, nm, 3sigma)	0.70	0.53	**0.5**

Table 3. AH data of five ASML imaging reticles. AFM data is measured on different patterns: HI (108 nm 4x horizontal isolated lines, pitch 616 nm), HD (80 nm 4x horizontal dense lines, pitch 176 nm), VI (116 nm 4x vertical isolated lines, pitch 616 nm), VD (100 nm 4x vertical lines, pitch 300 nm).

	Reticle A	Reticle B	Reticle C	Reticle D	Reticle E
AH average, blank data [nm]	70.5	70.5	69.5	70.1	70.1
AH variation, blank data, range over 4 measurements [nm]	0.1	0.1	0.1	0.4	0.4
AH average, AFM data [nm]	72.2 (HI) 72.3 (HD)		71.7 (HI)	72.0 (VD)	72.2 (VD)
AH variation, AFM data, 3sigma, 13x7 gratings within an image field, 5 locations within a 160x160 um^2 grating and 6 scans averaging [nm]	0.3 (HI) 0.4 (HD)		0.4 (HI)		
AH local variation, AFM data, 3sigma, 25 locations within 160x160 um^2 grating, 6 scans averaging [nm]	0.30 (HI) 0.25 (VI)		0.35 (HI) 0.67 (VI)		
AH variation, AFM data, 3sigma pooled, 2730 scans (HI), 9100 scans (HD), flyers removed [nm]	0.8 (HI) 0.7 (HD)		0.9 (HI)		
AH variation, AFM data, 3sigma, 13x7 locations within image field, 5 scans averaging [nm]				0.9 (VD)	0.6 (VD)

way to reduce the absorber volume is to apply negative line CD bias on the mask. NXE:3300 results show dose reduction of 10% per 1 nm (1x) reticle CD bias (Figure 2, Left). Contrast loss is not expected if the negative bias is applied. In particular, no line width roughness (LWR) increase or exposure latitude (EL) reduction is observed if CD bias is reduced by 2 nm (Figure 2, Center, Right). Dose gain of ~20% can be achieved if 14 nm (1x) reticle line CD is used instead of 16 nm for 16 nm half-pitch (hp) imaging.

A challenge is to achieve a good CD uniformity (CDU) and absorber profile control for thinner lines. Current ASML requirement for reticle CDU of 16 nm LS is 0.825 nm, 1x (3.3 nm, 4x) range over the image field.

2.3. Absorber height reduction allows for 10% dose gain

AH reduction can also allow for dose reduction, but can potentially result in contrast loss.[5][6][7] Simulations for 16 nm dense lines show that AH reduction from 70 nm to 54 nm allows for 13% dose gain with only a small contrast loss: 3% NILS (normalized intensity log-slope) (Figure 3, Left).

Simulation results sensitivity to details of absorber stack such as absorber optical constants and stack composition[7][8][12] does not allow determining optimal absorber with a better accuracy than ±1 nm. Experimental verification of simulation results is required.

It is demonstrated experimentally[7] that dose reduction of 8% can be achieved for 22 nm dense lines if AH is reduced from 72 nm to 52-54 nm (Figure 3, Right). In that study, optimal AH is found to be 52 nm for dense lines.

Based on the simulated and the experimental results, ~53 nm AH can be recommended for 16 nm imaging (an average between experimental and simulated optima). About 10% dose gain is expected as a result of AH reduction. Additional advantage of a thin absorber is an improved aspect ratio of mask structures allowing for further scaling.

There are several disadvantages of AH reduction such as tighter AH control and increased best focus shifts. They are described in subsequent sections.

2.4. Tight absorber height control is required

Tighter manufacturing AH control is required if AH is reduced. Based on the simulations the AH control (mean to target and variation) should be preferably within ±1 nm with corresponding NILS reduction up to 5%. This requirement should be compared with ITRS and current practical AH requirements and with actual performance.

ITRS (2013)[10] requirements for AH control are summarized in Table 1. The first uniformity requirement is based on wafer CDU impact (for 56 nm absorber mask); the other two are based on phase shifting properties of EUV absorber.[7][9]

The ITRS requirements are expressed in nanometers for 70 nm and 53 nm AH mask in year 2015 (Table 2). Current (2013-2014)

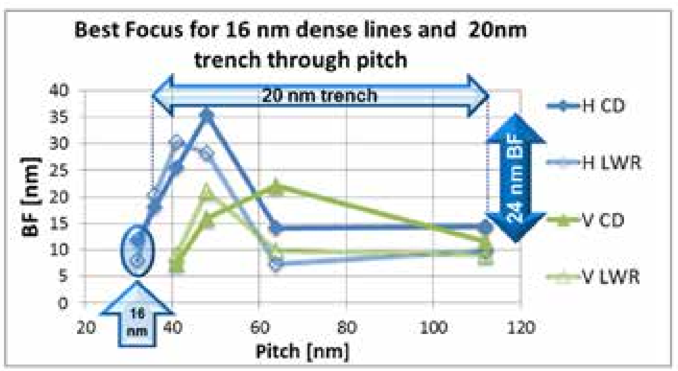

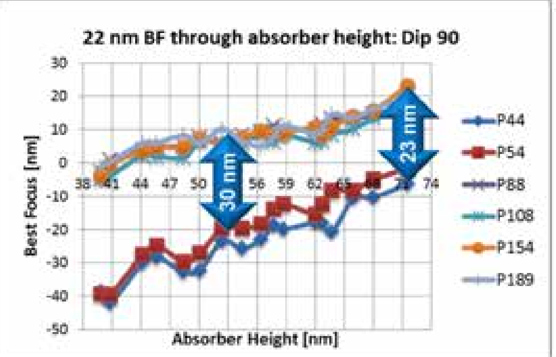

Figure 4. (Left) Best focus shifts for 16 nm dense lines and 20 nm trenches through pitch for a mask with 72 nm absorber. BF is determined based on 10% CD process window and based on LWR. Up to 24 nm BF range is observed through pitch. (Right) Experimental results[7] of 22 nm imaging through pitch and AH on NXE:3300 with Dipole 90Y illumination. AH reduction from 72 nm to 53 nm results in 7 nm BF range increase.

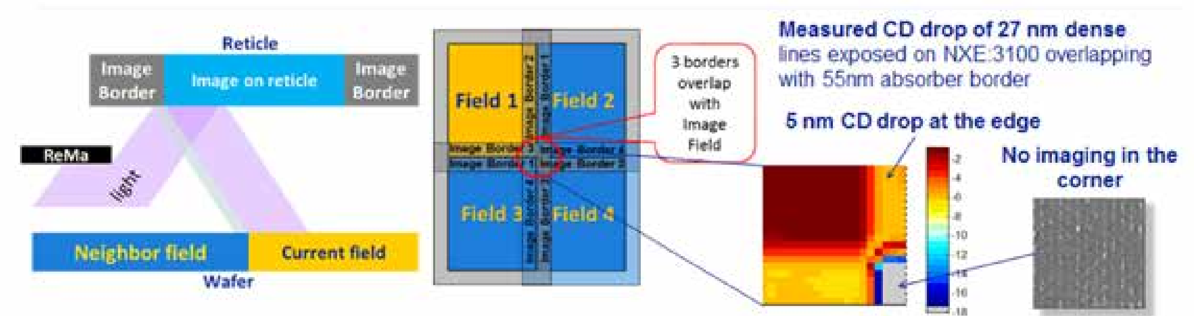

Figure 5. Die to die interactions on wafer. EUV light is reflected at the image border and impacts imaging in the neighboring die. In the corners of the dies reflections from the three neighboring image borders overlap with die area. 5 nm CD drop occurs for 27 nm dense lines at the edges of the field and no imaging is observed in the corners of the field if they overlap with 55 nm absorber border reflection of the neighboring fields.[14]

ASML requirements for AH control for imaging reticles are also added.

Based on the 16 nm simulations and ITRS requirements, ASML requirements may be tightened for thin absorber to 0.5 nm mean to target and 0.5 nm uniformity 3sigma.

Manufacturing accuracy of AH targeting might be insufficient. Blank data of five 70 nm ASML NXE:3300 imaging reticles shows that mean to target is within 0.5 nm (Table 3). This is a good performance satisfying the tight AH requirement (Table 2). However the absolute accuracy of AH determination at blank vendor is questionable as the blank vendor data contradict AFM data collected on a patterned mask. Detailed AFM (Bruker InSight) measurements on four of the reticles have shown about 1.7 to 2.2 nm positive offset with respect to requested 70 nm AH.[3] Absolute AFM calibration of ~1nm does not explain the observed offset. A negative offset w.r.t. the blank data might have been explained by the absorber loss during patterning; the positive offset is difficult to explain. As AFM measures the total step height, a part of the effect can be explained by overetching in Ru layer underneath during patterning. Another mechanism can be oxide layer growth.[7][8] As the Ta (per-) oxide density is smaller than of TaBO, the oxidation may effectively result in stack height increase.

Blank data is insufficient for determination of AH variation as only four measurements are provided.

Extensive AFM AH measurements were performed on several reticles[3] (Table 3). AH uniformity performance depends on sampling scheme. Local variation is below target 0.5 nm in most of the cases. Intrafield variation is below target 0.5 nm if enough scan and intragrating locations are measured and averaged. With only 5 scans averaging per location (the last two reticles), AH variation is close to the pooled distribution 3sigma. This proves that with a small amount of measurements per intrafield location, only local or metrology noise is captured.

2.5. Best Focus shifts and mitigation

There exists a trade-off between dose gain and best focus (BF) range increase through pitch if AH is reduced. It is shown experimentally[7] that AH reduction from 71 nm to 53 nm results in 7 nm BF range increase for 22 nm lines exposed with Dipole 90Y illumination. For 72 nm absorber, experimental BF range for 16 nm dense lines and 20 nm trenches through pitch is 24 nm,[3] i.e. we expect above 30 nm BF range for thinner absorber.

BF shifts are related to disbalance of diffraction orders. A possible mitigation strategy can be illumination source optimization. A usage of an optimized illumination or FlexPupil can improve depth of focus, process window and CDU.[11]

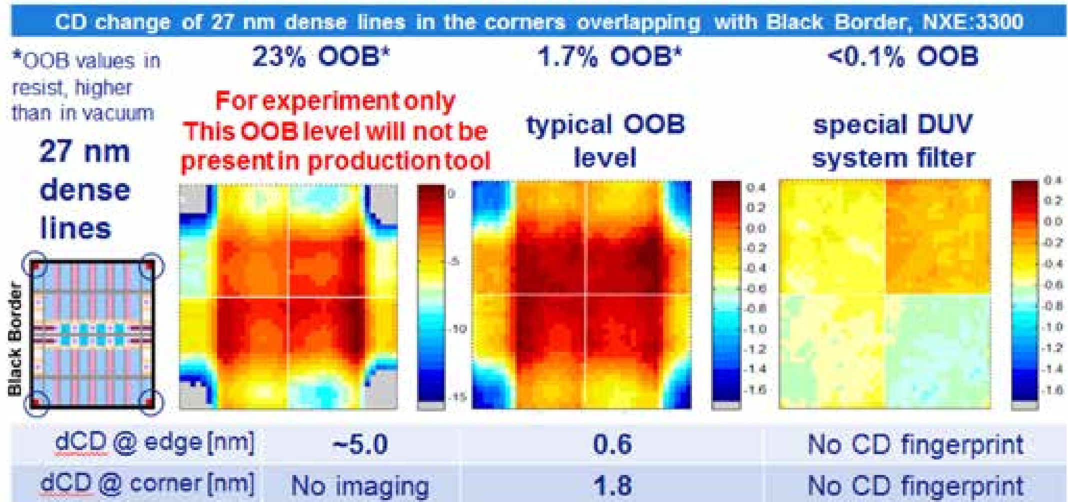

Figure 6. CD change of 27 nm dense lines in the corners overlapping with Black Border depends on OOB level in the scanner, NXE:3300 data.[15] OOB level is measured in resist and corrected for Al DUV reflectance (Eq (2)).

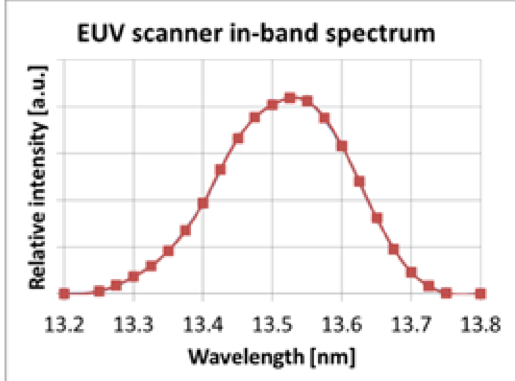

Figure 7. Estimated EUV scanner spectrum.

Table 4. Average reflectances of various EUV mask stacks are calculated based on reflectance spectra (Figure 8) and scanner spectrum (Figure 7).

Stack material	Average reflectance $R^{EUV}_{Material}$	$\frac{R^{EUV}_{Material}}{R^{EUV}_{ML}}$
72 nm abs on ML	1.2%	2.0%
84 nm abs on ML	0.18%	0.30%
184 nm abs on ML	0.09%	0.15%
84 nm abs + 100 nm Al on ML	0.02%	0.04%
57 nm TaBN+ 15 nm TaBO on LTEM	0.04%	0.07%
72 nm TaBN on LTEM	0.03%	0.05%
LTEM	0.02%	0.03%

3. Impact of DUV Black Border Reflections on Imaging

3.1. Field to field interactions and Black Border mitigation

The image border on a mask is a pattern free dark area surrounding the image field preventing exposure of the image field neighborhood on wafer. The regular EUV absorber 50-70 nm is not suitable for this purpose as it has 1-3% EUV reflectance resulting in 3-5 nm CD impact at the edge of the neighboring dies[13][14] (Figure 5).

Current widely accepted design of the black border on EUV reticle is an image border where the absorber and multilayer (ML) are etched down to the substrate (low thermal expansion material, LTEM) and EUV reflectance is reduced to <0.05%.[13] We have shown earlier[15] that the reflection of scanner DUV out-of-band light from BB results in essential CD change in a neighboring field: 0.6 nm at the edge and 1.8nm in the corner for typical OOB level (Figure 6). Similar results are demonstrated for contact holes.[18][19]

Specification for DUV and EUV reflections of Black Border are required to keep wafer CD under the control. These specifications can be derived if CD sensitivity to the reflected light is known and the level of background EUV and DUV light is measured or calculated.

3.2. DUV OOB light measurements

DUV Out-of-Band (OOB) light is measured in the scanner using a special test with a reticle containing a bright field ML area and an area coated with aluminum.[16] Al has very high DUV reflectance up to 90% for wavelengths above 190 nm and very low EUV reflectance <0.05%. The two parts of the reticle are exposed on the wafer with dose changing from field to field (dose meander) and dose to clear is determined. The OOB level is defined as the ratio of dose to clear from ML E_0^{ML} and the dose to clear from Al E_0^{Al}:

$$OOB_{Al} = \frac{E_0^{ML}}{E_0^{Al}}. \quad (1).$$

This number is higher than actual level of OOB in the scanner during normal exposure since both standard mask materials have lower DUV reflectance than Al: ML DUV reflectance R_{ML}^{DUV} is ~55% and absorber DUV reflectance is ~15% (see below for more details). The level of OOB in the scanner (e.g. Figure 6) is reported in terms of OOB from ML, i.e. corrected for high Al reflectance R_{Al}^{DUV}:

$$OOB_{ML} = OOB_{Al}\frac{R_{ML}^{DUV}}{R_{Al}^{DUV}}. \quad (2).$$

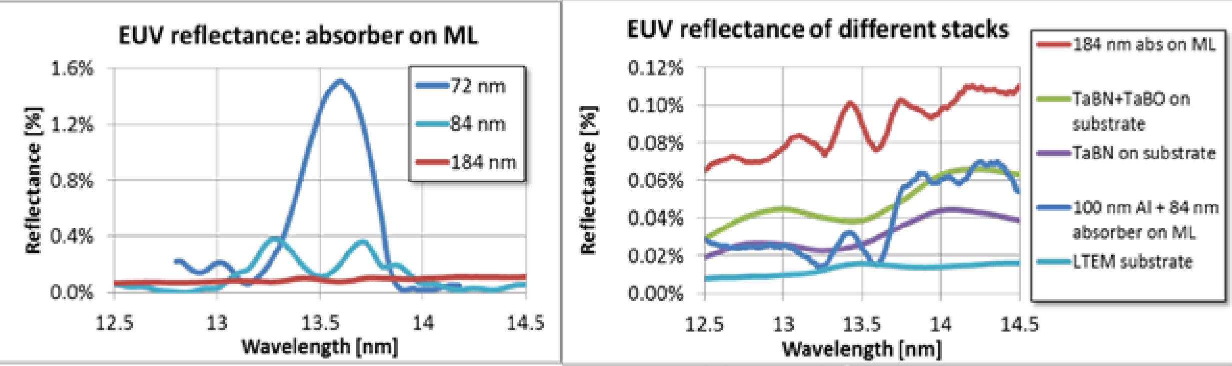

Figure 8. EUV reflectance spectra of different stacks measured at CXRO[21] and PTB[22]: (Left) absorber of 72 nm, 84 nm and 184 nm on ML; (Right) various low EUV reflectance stacks.

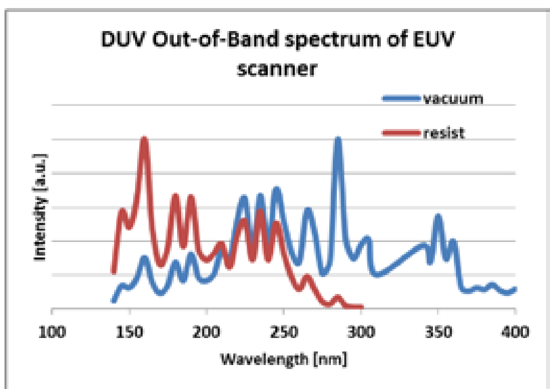

Figure 9. Estimated DUV OOB spectrum of EUV scanner.

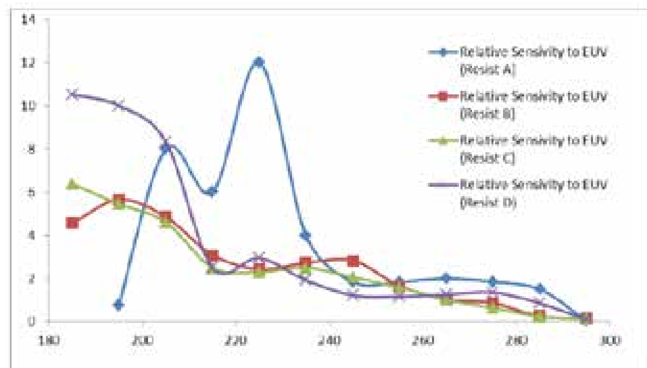

Figure 10. Relative resist DUV sensitivity through wavelength[20].

The OOB test is resist based. Since different resists have different OOB sensitivity, OOB level should be determined separately for each resist in question.[16][17]

3.3. Impact of reflections at the edge of the field

The following model is used for calculation of reflection impact on CD at the edge of the field:

$$\Delta CD = S^{EUV}\frac{R_{BB}^{EUV}}{R_{ML}^{EUV}} + S^{DUV}\,OOB_{Al}\frac{R_{BB}^{DUV}}{R_{Al}^{DUV}}. \qquad (3).$$

Here

- S^{EUV}[nm/%] is the CD sensitivity to background EUV light
- $\frac{R_{BB}^{EUV}}{R_{ML}^{EUV}}$ [%] is the percentage of background EUV light, calculated as the ratio of EUV reflectance R_{BB}^{EUV} of black border (or absorber image border) and EUV reflectance of ML R_{ML}^{EUV}
- S^{DUV}[nm/%] is the CD sensitivity to background DUV light;
- $OOB_{Al}\frac{R_{BB}^{DUV}}{R_{Al}^{DUV}}$ [%] is the percentage of background OOB light reflected from the black border, here R_{BB}^{DUV} is DUV reflectance of the black border (or absorber image border).

Determination of CD impact from black border reflections requires the knowledge of EUV reflectance from ML and BB and DUV reflectance of Al and BB.

3.4. Reflectance's of different stacks to EUV light

ML reflectance spectra are known from multiple publications (see e.g.[6][7][8][12]). Average ML EUV reflectance can be calculated using EUV scanner spectrum[6](Figure 7). The weighted average reflectance is about 60%.

The absorber reflectance depends on the absorber thickness and is also well known.[7][8][12] Thick absorber is proposed as an alternative solution for black border. The EUV reflectance determines whether this solution is feasible. The absorber reflectance's of thick absorbers averaged over the scanner spectrum are 1.2%, 0.18% and 0.09% respectively for 72 nm, 84 nm and 184 nm absorbers (Figure 8(Left), Table 4). The absorber stack reflectance is mostly caused by ML reflectance leaking through the absorber layer and modulated by light interference (swing curve). Even very thick absorber of 184 nm allows some EUV light through as its reflectance is larger than reflectance of absorber stacks coated directly on substrate (Figure 8 (Right), Table 4). Al and LTEM (ML etched BB) reflectance's are so low that they can be neglected in future considerations (Figure 8 (Right), Table 4).

3.5. Reflectance's of different stacks to DUV light

A scanner DUV out-of-band (OOB) spectrum is estimated based on source measurements in the plasma and scanner optics transmission to DUV light (Figure 9). EUV resists are not sensitive to DUV light above 300 nm,[16][20] the right part of the spectrum is therefore not relevant. Wavelengths below 140 nm could not be measured.

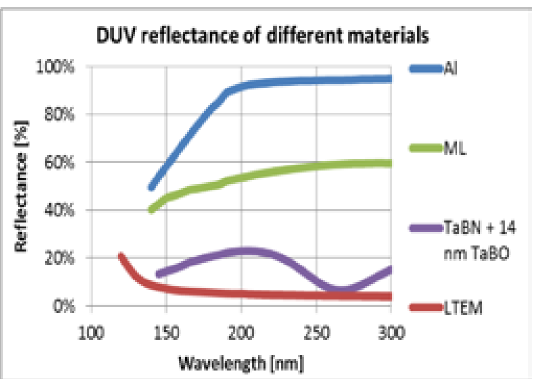

Figure 11. DUV reflectance spectra of different mask materials.

Table 5. Average DUV reflectances of different materials are calculated based on reflectance spectra (Figure 11) and scanner spectrum (Figure 9).

Material	Average refl in vacuum 115-130 nm	$\frac{R^{DUV}_{Material}}{R^{DUV}_{Al}}$ in vacuum	Average refl in resist 115-130 nm	$\frac{R^{DUV}_{Material}}{R^{DUV}_{Al}}$ in resist
Al	89%	1.0	71%	1.0
ML	55%	1.6	48%	1.5
TaBN+14 nm TaBO	15%	6.0	15%	4.6
LTEM	4.9%	18.1	7.3%	9.7

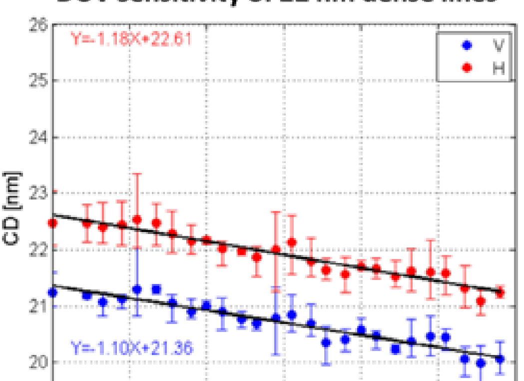

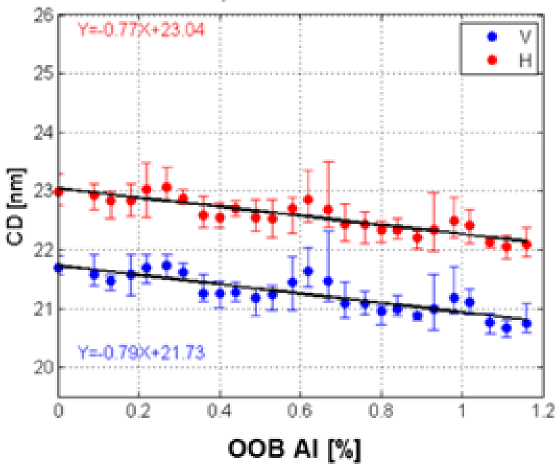

Figure 12. Experimental determination of DUV sensitivity by double exposure experiment, the second exposure is a dose meander with Al-coated reticle. (Left) DUV sensitivity of 22 nm dense lines (Horizontal and Vertical); (Right) DUV sensitivity of 22 nm isolated lines.

The spectrum is shown in vacuum and in resist. The latter is calculated using measured DUV sensitivity spectrum of a EUV resist (Resist C, Figure 10[20]) extrapolated to smaller wavelength. The spectrum in resist is clearly shifted to smaller wavelengths.

DUV reflectance's of different materials are shown in Figure 11. The average broad-band reflectance is calculated based on scanner DUV spectra (extrapolated to 115 nm) (Table 5). The average reflectance is essentially different in vacuum and in resist. Especially Al to LTEM (ML-etched BB) ratio is 1.9 times lower in resist because Al reflectance drops towards the smaller wavelengths while LTEM reflectance grows there. The knowledge of DUV scanner spectrum and DUV reflectance's at wavelengths down to 100 nm and below is absolutely required for thorough understanding of OOB impact on imaging. The availability of DUV spectrometers able to measure below 200 nm is very limited. Also understanding of DUV resist properties at lower DUV wavelengths and mitigation of their DUV sensitivity is of high importance.

3.6. CD sensitivity to EUV background light

CD sensitivity to background EUV light S^{EUV} is derived from experimental data,[15] it is 1.0±0.1 nm/% for dense lines and 0.8±0.1 nm/% for isolated lines. This sensitivity is almost independent of the imaging node.

3.7. CD sensitivity to DUV background light from Black Border

Determination of CD sensitivity to background DUV light S^{DUV} is less accurate, it is estimated to be 1.3±0.3 nm/% based on experimental data of a scanner with high level of DUV.[15] Here we investigate the DUV sensitivity in more detail.

A special test[17] is performed on NXE:3300 to determine the DUV sensitivity. A regular 22 nm imaging wafer is exposed second time with Al-coated reticle such that the dose changes from field to field (dose meander). CD changes through the dose of the second exposure and the obtained CD sensitivity is about 1.1-1.2 nm/% for dense lines and about 0.8 nm/% for isolated lines (Figure 12). The sensitivity is also determined through pitch (Figure 13, Left). This result is consistent with sensitivity of 27 nm dense lines 1.25nm/% (this value is derived based on data in[17]). The sensitivities are simulated using detailed scanner and reflectance spectra data and resist DUV properties (optical constants and sensitivity). The simulated sensitivities are very close to the measurements for isolated lines and slightly smaller 0.9-1.0 nm/% for dense lines

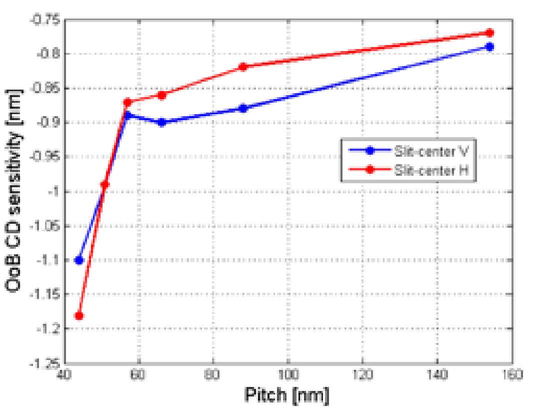

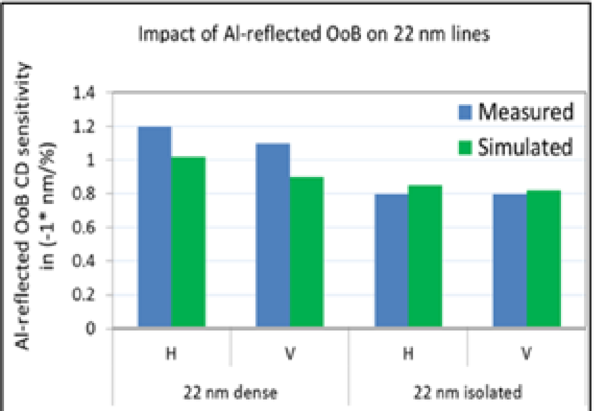

Figure 13. (Left) Experimentally determined DUV sensitivity for different pitches and two orientations. (Right) Comparison of measured and simulated DUV sensitivities for 22 nm dense and isolated H and V lines.

Table 6. OOB levels of EUV scanners at different conditions and corresponding CD drop of dense lines at the edge of imaging field.[15] Predicted CD drop is calculated using 1.1 nm/% DUV sensitivity. *High OOB levels were used for the experiment only and will not be present in an actual scanner.

OOB Al [%]	OOB ML [%]	OOB BB [%]	Measured ΔCD at the edge [nm]	Predicted ΔCD at the edge [nm]	Mismatch [nm]	Mismatch [%]
2.3	1.6	0.24	0.37	0.26	-0.10	-29
2.5	1.7	0.26	0.48	0.29	-0.17	-35
2.8	1.9	0.28	0.61	0.31	-0.32	-53
35*	24	3.6	4.0	4.0	0.0	0
39*	27	4.0	4.1	4.4	0.3	8
45*	30	4.6	5.0	5.1	0.1	2

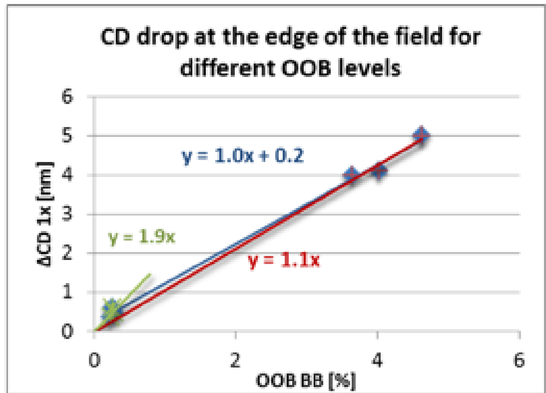

Figure 14.Calculation of CD sensitivity to DUV OOB light based on BB experimental data[15] (Table 6). The sensitivity based on high OOB levels is 1.0–1.1 nm/%, the sensitivity based on low OOB levels is 1.9 nm/%.

(Figure 13, Right). The sensitivities are also close to the sensitivities for EUV background light (Section 3.6).

3.8. Verification of CD impact caused by DUV reflections

The model (3) can be verified using available data of BB exposures (Figure 6[15], Table 6). Experimental DUV sensitivity 1.1 nm/% is used and OOB_{BB} level is calculated based on $\frac{R^{DUV}_{LTEM}}{R^{DUV}_{Al}}$ ratio in resist (Table 5).

Predictions match measurements quite well for high levels of OOB. For lower OOB levels, the predicted CD impact is much smaller than the observed values, in one of the cases the predicted value is twice smaller than the measured. A possible reason of the mismatch is unknown DUV resist sensitivity spectrum.

It is possible to estimate DUV sensitivity based on the measured data (Table 6). The sensitivity is calculated as a slope of ΔCD to OOB_{BB} (Figure 14). The sensitivity based on all data points is 1.0-1.1 nm/%; the sensitivity based on low OOB level only is almost twice higher 1.9 nm/%. If zero CD impact at zero OOB level is not included in data fit, ~0.2 nm CD impact is derived at zero OOB level. This effect is not understood.

Similar sensitivity results are obtained based on the data previously provided by Micron and imec (Table 7, see also[17][18][19]). OOB level of different resists is measured on imec NXE:3100 and CD drop of 27 nm dense lines is measured on the wafers with corresponding resists. The imec Al-test sensitivity of 1.25 nm/% is used for prediction. A systematic negative offset ~0.2 nm is observed between predicted and measured data. The sensitivity based on this data (Figure 15) is 1.19 nm/% which is very close to the Al-test based sensitivity. But if zero intercept is forced, the obtained sensitivity is much higher, 1.8 nm/%. This effect is not understood.

For practical application (e.g. for optical proximity correction (OPC) as mitigation strategy[18]) the understanding of CD impact at low DUV level is required. The study of DUV reflections on imaging will be continued.

3.9. DUV reflectance mitigation in the black border

CD impact of 0.6 nm at the edge and 1.8 nm in the corner (Figure 6) is considered to be too high and DUV reflectance mitigation strategy is required for the black border. A new improved type of black border is proposed with reduced DUV reflectance (Figure 16).

Current ASML specification for DUV BB reflectance is 6%; a target specification for the improved black border is 1.5% (or 4x

Table 7. OOB levels of different resists measured on imec NXE:3100 and corresponding CD drop in the corner and at the edge of imaging field. *Data is courtesy of Micron and imec.

Resist	OOB Al* [%]	OOB BB [%]	Measured ΔCD @corner* [nm]	Measured ΔCD @edge [nm]	Predicted ΔCD @edge [nm]
A	0.32	0.03	0.74	0.25	0.04
B	1.82	0.19	1.1	0.37	0.23
C	2.42	0.25	1.25	0.42	0.31
D	2.57	0.26	1.54	0.51	0.33
E	3.32	0.34	1.88	0.63	0.43

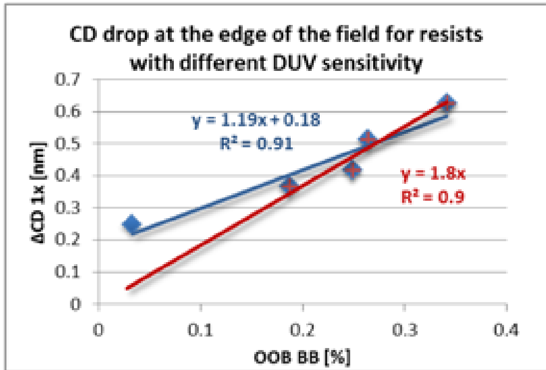

Figure 15. Calculation of CD sensitivity to DUV OOB light based on experimental data for different resists (Table 7[17]).

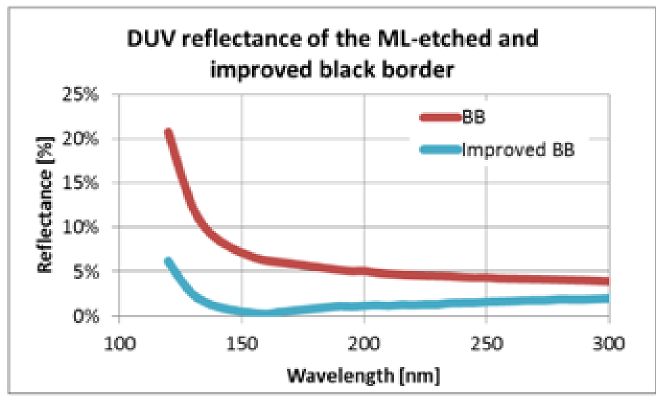

Figure 16. DUV reflectance spectra of the standard ML etched BB and an improved BB.

Table 8. Average DUV reflectance of standard BB and improved BB. Different averaging techniques are applied.

Averaging method	Uniform average			Spectrum in vacuum		Spectrum in resist	
Wavelength range [nm]	115-300	140-300	190-300	115-300	140-300	115-300	140-300
Standard BB reflectance [%]	6.2	5.0	4.0	4.9	4.6	7.3	5.4
Improved BB reflectance [%]	1.5	1.3	1.5	1.5	1.4	1.6	1.0
Ratio Standard vs Improved	4.1	3.8	2.7	3.3	3.3	4.6	5.4

reduction of reflectance). Average reflectance of the standard ML etched black border depends on the wavelength range and the way how the averaging is performed. It is not always practical to use the scanner OOB spectrum (Figure 9) for averaging, a simple uniform average can also be used (Table 8).

Practical uniform average reflectance of the standard and the improved BB is within the specification/target for 190-300 nm range (in air spectrometer) and for 140-300 nm (nitrogen atmosphere spectrometer), though the reduction of reflectance for improved BB is less than 4 times. Reflectance in resist for 115-190 nm range exceeds the specification, but the reduction ratio for improved BB is above 4x, which is considered as good performance of the improved black border.

3.10. Thick or double absorber as a black border

Thick or double absorber is another potential black border solution. Based on the model (3), measured reflectance ratio's (Table 5) and sensitivities (Figure 12), CD impact of thick absorber can be estimated as 1.0 nm at the edge and 3.0 nm in the corner for 84 nm absorber and 0.8 nm at the edge and 2.3 nm in the corner for 184 nm absorber.

$$\Delta CD = S^{EUV}\frac{R^{EUV}_{BB}}{R^{EUV}_{ML}} + S^{DUV}OOB_{ML}\frac{R^{DUV}_{Al}}{R^{DUV}_{ML}}\frac{R^{DUV}_{BB}}{R^{DUV}_{Al}} = 1.0\frac{nm}{\%}0.3\% + 1.1\frac{nm}{\%}1.7\%\cdot 1.5\cdot\frac{1}{4.6} \approx 1.0\,nm \quad 4.$$

These values are too high and thick/double absorber cannot serve as a black border. It is proposed[18] that this mitigation strategy is combined with OPC correction; REMA (Reticle Masking blades) accuracy of ±15 um is required for 84 nm absorber border and this requirement can be further relaxed if the absorber is

Table 9. Advantages and disadvantages of absorber optimization for imaging dose reduction.

Absorber volume optimization strategy	Negative reticle line CD bias	Absorber height reduction
Description	2 nm negative bias, line CD 14 nm 1x	Reduction from 70 nm to 53 nm
Dose gain	~10% per 1 nm (1x) reticle CD ~20% in total	~10%
Contrast impact	No LWR increase or EL reduction is observed	Expected small contrast loss (3-5% NILS)
Additional advantages	-	Improved aspect ratio absorber height vs line CD; a better scaling extendibility.
Challenges	CDU and absorber profile control for thinner lines	Tighter mean to target and uniformity absorber height control (down to 0.5 nm)
Disadvantages	-	Increased best focus range through pitch
Additional requirements	-	Extensive absorber height metrology before and after patterning; absorber height specification on patterned reticle

thicker. However there are also other manufacturability drawbacks of double absorber mitigation strategy such as more complicated process, impact on resolution, pattern degradation and increased defectivity. ML etched black border is therefore still considered as the best option.

4. Summary

Two important aspects of EUV mask architecture is covered in this work. Imaging dose reduction is required for 16 nm hp imaging. Reduction of absorber height volume on the mask (negative line CD bias and absorber height reduction) is a possible option for imaging dose reduction up to 30%. Advantages and disadvantages of the proposed techniques are summarized in Table 9.

If both techniques are applied dose for 16 nm imaging can be reduced by ~30% from 55 mJ/cm^2 to about 38 mJ/cm^2.

In the second part of this work a systematic approach to black border reflections impact on imaging is established. Impact on CD is calculated as a product of EUV and DUV relative background light and CD sensitivity to this light. The relative background light is calculated based on measured OOB DUV level in the system and measured broadband reflectance's of different mask materials. The need of low DUV wavelength reflectance metrology (in the range 100-300 nm) is demonstrated using an estimated NXE scanner out-of-band DUV spectrum. CD sensitivity to EUV and DUV light is determined. The model is verified based on wafer data collected on NXE:3300 and NXE:3100 systems for 22 nm and 27 nm dense lines. The observed impact of black border on imaging is larger than predicted for low OOB levels. This effect is still to be understood. DUV reflectance specification <1.5% is required for black border in order to mitigate the impact on imaging. Promising results of low DUV reflectance of the black border are shown.

5. Acknowledgments

The authors would like to thank their ASML colleagues Bert Vleeming for the support of this project, Koen van Ingen Schenau, John McNamara, Thijs Hollink, Joost Hageman, Andre van Dijk for fruitful discussions, Vidya Vaenkatesan and Wendy Liebregts for extensive metrology, Rik Hoefnagels for provided resist information, Katrin Letz for facilitation of reticle manufacturing and measurements, Laurens de Winter for simulation support and many others for good discussions and inspiring atmosphere of cooperation. We would like to thank Toppan Photomasks colleagues for the continuous support: Romy Wende, Renée-Paule Lefebvre, Franklin Kalk and colleagues from Toppan Printing: Isao Yonekura and Hidemitsu Hakii. A special thank is for Ardavan Niroomand from Micron, Rik Jonckheere, Eric Hendrickx and Gian Lorusso from imec for the provided data on resist DUV sensitivity and imaging impact. A special thank is for Rafael Howell and his colleagues from ASML Brion for the information about SMO capabilities.

6. References

[1] Peeters, R. et al., "EUV lithography: NXE platform performance overview," **Proc. SPIE 9048,** Extreme Ultraviolet (EUV) Lithography V, 90481J (2014).

[2] van Setten, E. et al., "Imaging performance and challenges of 10nm and 7nm Logic nodes with 0.33 NA EUV," **Proc. SPIE 9231,** 923118 (2014).

[3] Davydova, N.V. et al., "Achievements and challenges of EUV mask imaging," **Proc. SPIE 9256,** 925644 (2014).

[4] van den Horst, J.W. et al., "Performance overview of ASML's NXE platform," **Proc. SPIE 9231** (2014).

[5] Davydova, N.V., van Setten, E., de Kruif, R., Oorschot, D., Dusa, M., Wagner, C., Jiang, J., Liu, W., Kang, H., Liu, H., Spies, P., Wiese, N., and Waiblinger, M., "Imaging performance improvements by EUV mask stack optimization," **Proc. SPIE 7985,** 79850X (2011).

[6] Davydova, N.V., van Setten, E., Han, S.-I., van de Kerkhof, M., de Kruif, R., Oorschot, D., Zimmerman, J., Lammers, A., Connolly, B., Driessen, F., van Oosten, A., Dusa, M., van Dommelen, Y., Harned, N., Jiang, J., Liu, W., Kang, H., and Liu, H.-Y., "Mask aspects of EUVL imaging at 27nm node and below," **Proc. SPIE 8166,** 816624 (2011).

[7] Davydova, N.V., Kruif, R.C., Rolff, H., Connolly, B., van Setten, E., Lammers, A., Oorschot, D., Fukugami, N., and Kodera, Y., "Experimental approach to EUV imaging enhancement by mask absorber height optimization," **Proc. SPIE 8886,** 888622 (2013).

[8] Davydova, N.V., de Kruif, R.C., van Setten, E., Connolly, B., Mehagnoul, K., Zimmerman, J., Harned, N., Kalk, F., "EUVL mask performance and optimization," **Proc. SPIE 8352,** 835208 (2012).

[9] Murachi, T., Tanabe, H., Park, S.J., Gullikson, E., Ogase, T., Abe, T., Hayashi, N., "Direct phase-shift measurement of thin and thick absorber EUV masks," **Proc. SPIE 8441,** 84411M (2012)

[10] http://www.itrs.net/Links/2013ITRS/Home2013.htm

[11] Liu, X. et al., "EUV source-mask optimization for 7 nm node and beyond," **Proc. SPIE 9048,** 90480Q (2014).

[12] Philipsen, V., Hendrickx, E., Jonckheere, R., Davydova, N., Fliervoet, T., and Neumann, J.T., "Actinic characterization and modeling of the EUV mask stack," **Proc. SPIE 8886,** 888619 (2013).

[13] Fukugami, N., Matsui, K., Watanabe, G., Isogawa, T., Kondo, S., Kodera, Y., Sakata, Y., Akima, S., Kotani, J., Morimoto, H., and Tanaka, T. "Black border with etched multilayer on EUV mask," **Proc. SPIE 8441,** 84411K (2012).

[14] Davydova, N.V., de Kruif, R.C., Fukugami, N., Kondo, S., Philipsen, V., van Setten, E., Connolly, B., Lammers, A., Vaenkatesan, V., Zimmerman, J., and Harned, N., "Impact of an etched EUV mask black border on imaging and overlay," **Proc. SPIE 8522**, 852206 (2012).

[15] Davydova, N.V. et al., "Impact of an etched EUV mask black border on imaging. Part II," **Proc. SPIE 8880,** 888027 (2013)

[16] Lorusso, G. F., Davydova, N., Eurlings, M., Kaya, C., Peng, Y., Feenstra, K., Fedynyshyn, T. H., Natt, O., Huber, P., Zaczek, C., Young, S., Graeupner, P., and Hendrickx, E.,"Deep Ultraviolet Out-of-Band Contribution in Extreme Ultraviolet Lithography: Predictions and Experiments," **Proc. SPIE 7969,** 79692O (2011).

[17] Lorusso, G.F., Matsumiya, T., Iwashita, J., Hirayama, T., and Hendrickx, E., "Deep ultraviolet out-of-band characterization of EUVL scanners and resists," **Proc. SPIE 8679,** Extreme Ultraviolet (EUV) Lithography IV, 86792V (2013).

[18] Maloney, C. et al., "Feasibility of compensating for EUV field edge effects through OPC," **Proc. of SPIE 9048, 90480T** (2014).

[19] Gao, W. et al., "Study of CD variation caused by the black border effect and out-of-band radiation in extreme ultraviolet lithography," *J. Micro/Nanolith. MEMS MOEMS 13(2),* 023005 (2014).

[20] Liping, R. et al., "ASML Alpha Demo Tool Out-of-Band Radiation Evaluation," EUVL (2011).

[21] http://cxro.lbl.gov/

[22] http://www.ptb.de/mls/aufgaben/euvreflectometry.html

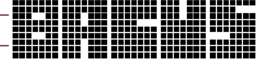

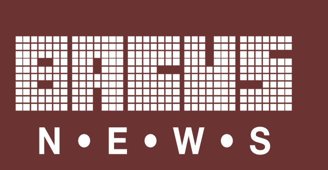

N • E • W • S

Sponsorship Opportunities

Sign up now for the best sponsorship opportunities

Photomask 2014 —
Contact: Lara Miles, Tel: +1 360 676 3290; laram@spie.org

Advanced Lithography 2015 —
Contact: Teresa Roles-Meier,
Tel: +1 360 676 3290; teresar@spie.org

Advertise in the BACUS News!

The BACUS Newsletter is the premier publication serving the photomask industry. For information on how to advertise, contact:

Lara Miles
Tel: +1 360 676 3290
laram@spie.org

BACUS Corporate Members

Acuphase Inc.
American Coating Technologies LLC
AMETEK Precitech, Inc.
Berliner Glas KGaA Herbert Kubatz GmbH & Co.
FUJIFILM Electronic Materials U.S.A., Inc.
Gudeng Precision Industrial Co., Ltd.
Halocarbon Products
HamaTech APE GmbH & Co. KG
Hitachi High Technologies America, Inc.
JEOL USA Inc.
Mentor Graphics Corp.
Molecular Imprints, Inc.
Panavision Federal Systems, LLC
Profilocolore Srl
Raytheon ELCAN Optical Technologies
XYALIS

Industry Briefs

Global Chip Sales Hit Record in June

By **Ismini Scouras,** EEtimes

Improved economic conditions worldwide, particularly in the U.S., and a booming memory chip market are being credited for the global semiconductor industry's robust sales growth in the first half of 2014.

According to the latest numbers compiled by the World Semiconductor Trade Statistics (WSTS), global sales in June grew 10.8%, to $27.57 billion from $24.88 billion in June 2013, and 2.6% from $26.86 billion in May. June's numbers represent the industry's highest monthly sales level recorded, according to the SIA.

In the second quarter of 2014, worldwide chip sales reached $82.7 billion, up 10.8% from the second quarter of 2013, and 5.4% sequentially. Global sales were up 11.1% in the first half of 2014 compared to the same period in 2013, which was a record year for semiconductor revenue. WSTS projects growth of 6.5% in 2014, 3.3% in 2015, and 4.3% in 2016, said SIA President and CEO Brian Toohey.

Memory products, including DRAM, have been one of the strongest sectors. In June, DRAM was up 29.2% compared to June 2013, analog was up 13.5%, and logic was up 12.1%, according to the WSTS figures.

Geographically, the Americas posted the largest sequential gains in June, growing 4.9 percent compared with May 2014. Semiconductor sales in Asia-Pacific, as well as Japan, grew 2.1%, and Europe inched up 1.9%. And the gains were even larger compared to June 2013 as sales increased 12.1% in both the Americas and Europe, 10.5% in Asia Pacific, 8.5% in Japan.

2-Year Chipmaking Equipment Spending Boom Coming

By **Peter Clarke,** EEtimes

After years of underspending on chipmaking equipment, the semiconductor equipment industry is set for two consecutive strong growth years, according to the SEMI industry organization. The SEMI trade body is forecasting the global market will grow by 20.8 percent in 2014 to reach $38.4 billion and to expand another 10.8 percent in 2015 to exceed $42.6 billion.

All the regions of the world that SEMI tracks separately are forecast to see equipment spending increases in 2015. Front-end wafer processing equipment is forecasted to grow 11.9 percent in 2015 to $34.8 billion, up from $31.1 billion in 2014. Test equipment and assembly and packaging equipment is predicted to experience growth next year, rising to $3.1 billion (+1.6%) and $2.6 billion (+1.2%), respectively. The forecast indicates that next year is on track to be the second largest spending year ever, surpassed only by $47.7 billion spent in 2000.

Growth is forecasted in all regions except ROW in 2014 and all regions in 2015. Taiwan is forecast to continue to be the world's largest spender with $11.6 billion estimated for 2014 and $12.3 billion for 2015. In 2014, North America is second at $7.2 billion, followed by South Korea at $6.9 billion. For 2015, South Korea is in second ($8.0 billion) in spending, followed by North America ($7.3 billion).

In 2014, year-over-year increases are expected to be largest for China (47.3 percent), North America (35.7 percent), South Korea (33.0 percent), and Europe (29.7 percent). Year-over-year percentage increases for 2015 are largest for Europe (47.8 percent increase), ROW (23.5 percent), Japan (15.6 percent), and South Korea (15.0 percent).

Join the premier professional organization for mask makers and mask users!

About the BACUS Group

Founded in 1980 by a group of chrome blank users wanting a single voice to interact with suppliers, BACUS has grown to become the largest and most widely known forum for the exchange of technical information of interest to photomask and reticle makers. BACUS joined SPIE in January of 1991 to expand the exchange of information with mask makers around the world.

The group sponsors an informative monthly meeting and newsletter, BACUS News. The BACUS annual Photomask Technology Symposium covers photomask technology, photomask processes, lithography, materials and resists, phase shift masks, inspection and repair, metrology, and quality and manufacturing management.

Individual Membership Benefits include:

- Subscription to BACUS News (monthly)
- Eligibility to hold office on BACUS Steering Committee

www.spie.org/bacushome

Corporate Membership Benefits include:

- 3-10 Voting Members in the SPIE General Membership, depending on tier level
- Subscription to BACUS News (monthly)
- One online SPIE Journal Subscription
- Listed as a Corporate Member in the BACUS Monthly Newsletter

www.spie.org/bacushome

Calendar

2014

SPIE Photomask Technology
Co-located with
SPIE Scanning Microscopies
16-18 September 2014
Monterey Marriott and
Monterey Conference Center
Monterey, California, USA
www.spie.org/pm

SPIE Scanning Microscopies
Co-located with
SPIE Photomask Technology
16-18 September 2014
Monterey Marriott and
Monterey Conference Center
Monterey, California, USA
www.spie.org/sg

2015

SPIE Advanced Lithography
22-26 February 2015
San Jose Convention Center
and San Jose Marriott
San Jose, California, USA
www.spie.org/al

SPIE is the international society for optics and photonics, a not-for-profit organization founded in 1955 to advance light-based technologies. The Society serves nearly 225,000 constituents from approximately 150 countries, offering conferences, continuing education, books, journals, and a digital library in support of interdisciplinary information exchange, professional growth, and patent precedent. SPIE provided over $3.2 million in support of education and outreach programs in 2013.

SPIE.

International Headquarters
P.O. Box 10, Bellingham, WA 98227-0010 USA
Tel: +1 360 676 3290
Fax: +1 360 647 1445
help@spie.org • www.SPIE.org

Shipping Address
1000 20th St., Bellingham, WA 98225-6705 USA

Managed by SPIE Europe
2 Alexandra Gate, Ffordd Pengam, Cardiff,
CF24 2SA, UK
Tel: +44 29 2089 4747
Fax: +44 29 2089 4750
spieeurope@spieeurope.org • www.spieeurope.org

You are invited to submit events of interest for this calendar. Please send to lindad@spie.org; alternatively, email or fax to SPIE.